GEOPHYSICS, VOL. 68, NO. 2 (MARCH-APRIL 2003); P. 685–689, 5 FIGS.
10.1190/1.1567239

Short Note

Microseismic monitoring of borehole fluid injections: Data modeling and inversion for hydraulic properties of rocks

Elmar Rothert* and Serge A. Shapiro*

INTRODUCTION

Attention paid to microseismic monitoring during geothermal or hydrocarbon reservoir operations has grown considerably over the last several years. The observation of microseismicity occurring during borehole fluid injections or extractions has a large potential in characterizing reservoirs at locations as far as several kilometers from boreholes (Talwani and Acree, 1985; Adushkin et al., 2000; Fehler et al., 2001). The most common application has been hydraulic fracture imaging and growth characterization (e.g., Phillips et al., 1997; Urbancic et al., 1999). Longer-term microseismic monitoring has been used to map oil-producing natural fractures (e.g., Rutledge et al., 1998); it also shows promise in tracking flood fronts in the case of enhanced oil recovery (e.g., Maxwell et al., 1998). Beyond delineating conductive fracture geometry and inferring fluid-flow paths, microseismic data could potentially be used to measure in-situ hydraulic properties of rocks at interwell scales, providing information that could further guide operations to optimize field production.

Recently, an approach for the interpretation of microseismic data was proposed to provide in-situ estimates of the hydraulic diffusivity characterizing a geothermal or hydrocarbon reservoir on the large spatial scale (on the order of 10^3m). This approach, called seismicity-based reservoir characterization (SBRC), uses a spatio-temporal analysis of fluid injection-induced microseismicity to reconstruct the tensor of hydraulic diffusivity and to estimate the tensor of permeability [see Shapiro et al. (1997, 1999, 2000, 2002) and the discussion of the method in Cornet (2000)]. The approach assumes the following main hypothesis: Fluid injection in a borehole causes perturbations of the pore pressure in rocks. Such perturbations cause a change of the effective stress, which, if large enough, can trigger earthquakes along preexisting zones of weakness. The SBRC approach considers that most of the seismicity is triggered along critically stressed, preexisting fractures.

In agreement with this main hypothesis, the SBRC approach introduces one more assumption: the spatio-temporal evolution of the hydraulic-induced microseismicity is completely defined by the diffusion-like process of pore-pressure relaxation. The analysis of spatio-temporal features of the microseismicity then provides a possibility to invert for hydraulic diffusivity distributions in fluid-saturated rocks. The approach has been successfully applied to real data several times (Shapiro et al., 2000; Rothert et al., 2001; Audigane et al., 2002; Shapiro et al., 2002). In this paper, we present an approach for the numerical modeling of microseismicity to verify the SBRC method. In spite of the apparent simplicity of this approach, it reproduces significant features of microseismicity observed in reality. We consider this an additional indication that our description of the main physical features of the triggering phenomenon are adequate. Then we focus on the verification of the SBRC inversion algorithms using synthetic data.

A SUMMARY OF THE SBRC CONCEPT

In the low-frequency limit of the Biot equations of poroelasticity (Biot, 1962), the pore-pressure perturbation p can be approximately described by the following differential equation of diffusion:

$$\frac{\partial p}{\partial t} = \frac{\partial}{\partial x_i}\left[D_{ij}\frac{\partial}{\partial x_j}p\right]. \tag{1}$$

Here, D_{ij} are the components of the tensor of hydraulic diffusivity, x_j ($j = 1, 2, 3$) are the components of the radius vector from the injection point to an observation point, and t is time. Equation (1) corresponds to the second-type Biot wave (the slow P-wave) in the limit of the frequency being extremely low in comparison with the global-flow critical frequency (Biot, 1962). The tensor of hydraulic diffusivity is directly proportional to the tensor of the permeability (see Shapiro et al., 2002).

Published on Geophysics Online August 19, 2002. Manuscript received by the Editor February 8, 2002; revised manuscript received August 15, 2002.
*Freie Universität Berlin, Fachrichtung Geophysik, Malteserstr. 74-100, Build. D, D-12249 Berlin, Germany. E-mail: rothert@geophysik.fu-berlin.de; shapiro@geophysik.fu-berlin.de.

Considering the power spectrum of a step-function injection signal, which can roughly approximate a real pore-pressure perturbation, Shapiro et al., (1997, 2000) introduce a heuristic concept of the microseismic triggering front. This front is regarded as a spatial surface which separates the regions of the relaxed and unrelaxed pore pressure perturbation. For example, in the case of a homogeneous and isotropic medium, Shapiro et al. (1997) obtained the following equation describing the spatial position, r, of the triggering front in an effective isotropic homogeneous poroelastic medium with the scalar hydraulic diffusivity D:

$$r = \sqrt{4\pi Dt}. \tag{2}$$

Equation (2) is able to provide scalar, homogeneous estimates of the hydraulic diffusivity only. For the case of a heterogeneously distributed D and a step-function pressure perturbation, an eikonal-like equation is derived which describes the triggering time $t(\mathbf{r})$ (see Shapiro et al., 2002):

$$|\nabla t|^2 = \frac{t}{\pi D}. \tag{3}$$

This equation was derived using an approximation based on geometrical optics, which is a heuristic treatment of the diffusion equation with a heterogeneous diffusion coefficient. Equation (3) serves as a basis for the inversion procedure to reconstruct spatial distributions of the hydraulic diffusivity in heterogeneous media.

Because equations (2) and (3) both were derived in a quasi-heuristic way, a quantitative approach is required to verify the inversion algorithms based on them. A possible method of verification is to apply the inversion algorithms to numerically simulated microseismic data. For this approach a numerical simulation of microseismicity during borehole fluid injections is required.

NUMERICAL SIMULATIONS OF THE TRIGGERING PHENOMENON

The variety of possible mechanisms responsible for microearthquake triggering by borehole fluid injections is still to be understood. For example, during massive hydraulic injections, hydrofracturing may be a reason for releasing microseismicity (Urbancic et al., 1999). Dvorkin and Nur (1992) propose an alternative model of hydrofracturing, where the filtration front opens many new microcracks. Such a phenomenon can also be a reason of microseismicity in the case of large pressure perturbations. However, in many cases the pore-pressure variations are too small to create new fractures far from boreholes [e.g., during an injection experiment in 1994 at the KTB site in Germany. Such variations were maximum 1% larger than the hydrostatic pressure (see Zoback and Harjes, 1997)]. Thus, we assume that a diffusive process of pore pressure relaxation reducing the effective normal stress and leading to an activation of motion along critical cracks might be the dominant reason for triggering microseismicity (see also Hubbert and Rubey, 1959; Pearson, 1981). This hypothesis is the basis of the SBRC approach.

To model the triggering of microseismicity numerically, we simulate the process of pore pressure relaxation in a medium with statistically distributed critical zones. We use a finite-element (FE) algorithm to solve the time-dependent parabolic equation of diffusion for a 2D homogeneous, isotropic background medium with the source point located in the center of the model (Figure 1). As an input signal, a step function such as pressure perturbation with constant amplitude P_0 is

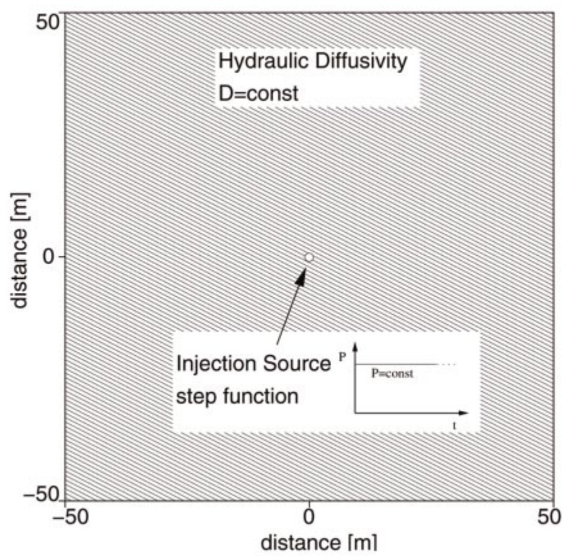

(a)

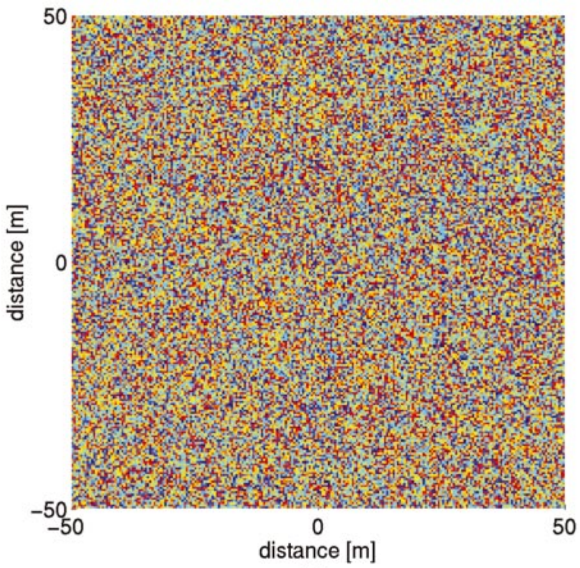

(b)

FIG. 1. (a) Sketch of a 2D model used for numerical tests. The dimensions of the model are 100×100 m. The scalar hydraulic diffusivity $D = 1$ m^2/s is distributed homogeneously in space. The injection source is located at the center of the model. The step-function time dependence of the pressure perturbations is shown. (b) The distribution of the failure criterion. The medium is divided into 426×426 cells. Within each cell a random value of critical pore pressure is assigned which, once exeeded, triggers a microseismic event. Color denotes the value of the failure criterion: blue corresponds to highly critical locations (i.e., locations with a low critical pressure) and red denotes stable zones.

used. After obtaining the solution of the pressure perturbation within the medium for a modeling time (100 s in this case), we divide the medium into small cells. A failure criterion (trigger criterion) is then randomly distributed in space. It is also statistically distributed within a given range of pressure amplitude. This procedure directly follows the concept of the SBRC approach: that real rocks are in a subcritical state of stress in some places. Triggering occurs at points where the amplitude of pore pressure perturbation exceeds the failure criterion. This procedure allows one to obtain synthetic microseismicity clouds. Also, the spatio-temporal evolution of the events resulting from pore-pressure variation can be studied. An example for a randomly distributed failure criterion is shown in Figure 1b. In this case, the triggering criterion is distributed normally between zero and a maximum criticality value ($10 \cdot P_0$ in this model).

Figure 2a shows the result of the modeling. The synthetic cloud of events generated during 100 s of numerically simulated fluid injection consists of 2636 events. In Figure 2b the estimation of the scalar hydraulic diffusivity using equation (2) is shown for the data set of Figure 2a. It is obvious that the spatio-temporal distribution of the events agrees very well with the behavior predicted by equation (2) in spite of the heuristic character of this equation. The triggering front corresponding to the value of diffusivity used in the homogeneous model ($D = 1$ m^2/s) is indicated by the solid line according to equation (2). Located below this line are 95.7% of all events triggered.

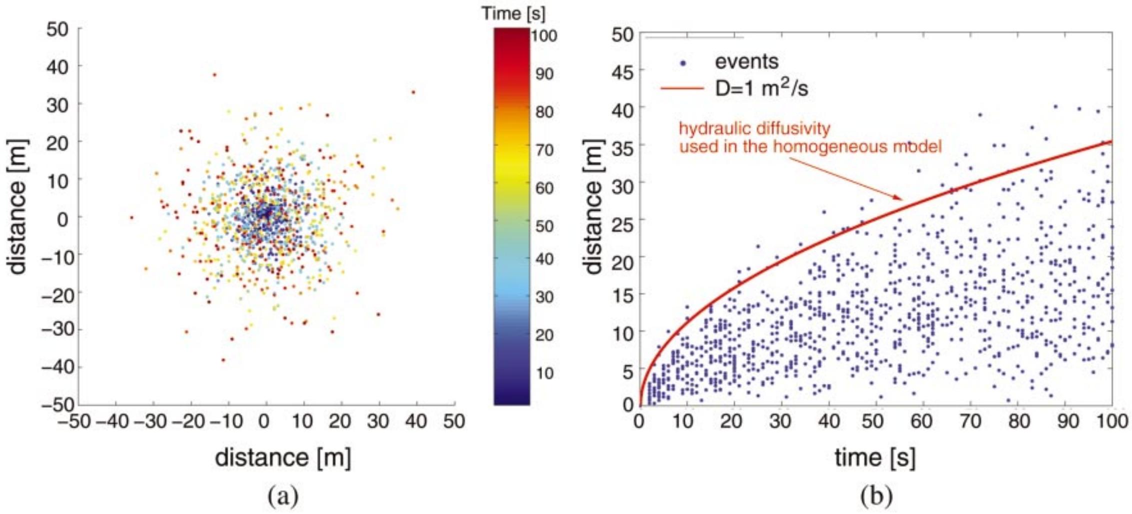

FIG. 2. (a) Synthetic cloud of events resulting from the model shown in Figure 1. Color denotes the event occurrence time. (b) Estimation of scalar hydraulic diffusivity using synthetic events shown in (a). The solid line corresponds to equation (2), with the value of hydraulic diffusivity $D = 1$ m^2/s.

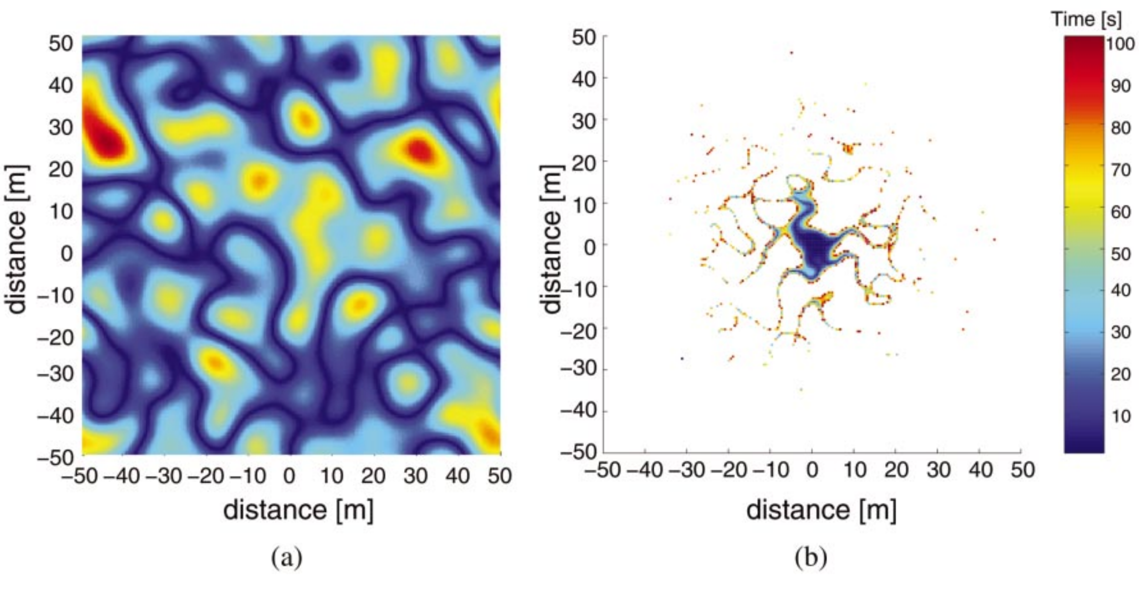

FIG. 3. (a) Triggering criterion with a Gaussian autocorrelation function. As in Figure 1b, the color corresponds to the criticality of the medium. (b) Synthetic cloud of events resulting from modeling using the failure criterion shown in (a). Exactly 1984 events were triggered during the first 100 s of the injection simulation.

It is also interesting to see that in spite of apparent simplicity of this modeling approach, the synthetic cloud of events shows several important characteristic features of microseismic clouds obtained in reality. First, it has a characteristic parabolic envelope [compare this with Figure 2 from Shapiro et al. (2002) where real data are plotted]. Second, a parabolic zone of low event density (see, e.g., Figure 2b, a strip of low event density for distances smaller than 5 m) looking like a back triggering front also can be usually observed in reality [compare again with Figure 2 of Shapiro et al. (2002)].

By using different probability-density types for the failure criterion as well as correlating it spatially (e.g., with Gaussian or exponential autocorrelation functions), the influence of different types of criticality statistics on the triggering process can be studied. For example, a structure of critical zones can be included in the models. In Figure 3a, a Gaussian-correlated distribution of the trigger criterion is simulated. The synthetic event cloud is shown in Figure 3b. Events are clustered along major critical zones in the medium. Details of our study of criticality statistics' influence on the triggering process are beyond the scope of this study.

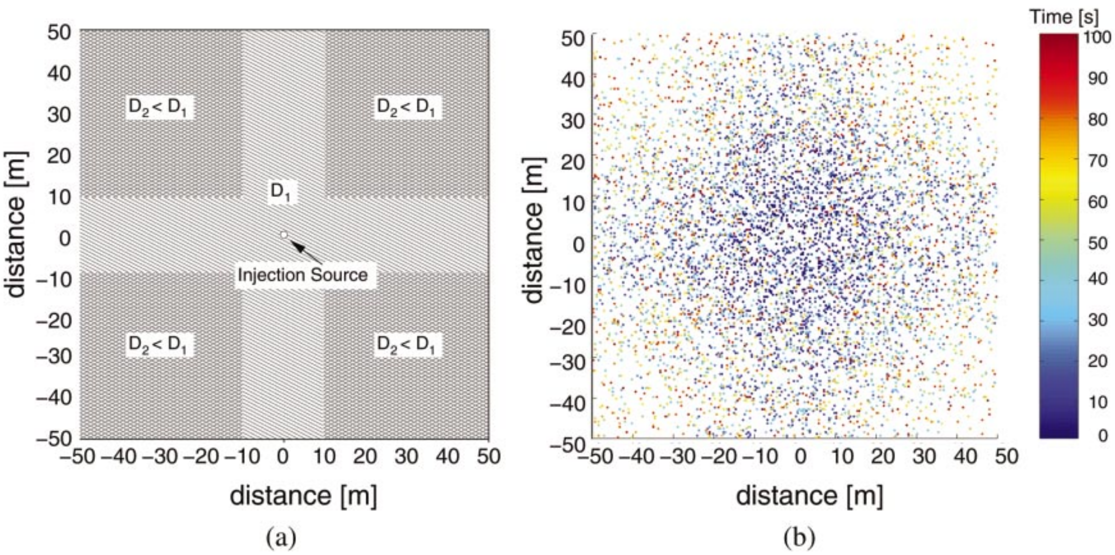

FIG. 4. (a) Sketch of a hydraulically heterogeneous model. The value of hydraulic diffusivity in the inner cross-shaped structure is $D_1 = 50$ m^2/s, whereas its value in the surrounding regions is ten times smaller ($D_2 = 5$ m^2/s). (b) Synthetic cloud of events for the heterogeneous model from Figure 4a and the failure criterion shown in Figure 1b. Exactly 20 337 events were triggered. The color corresponds to the event occurrence time.

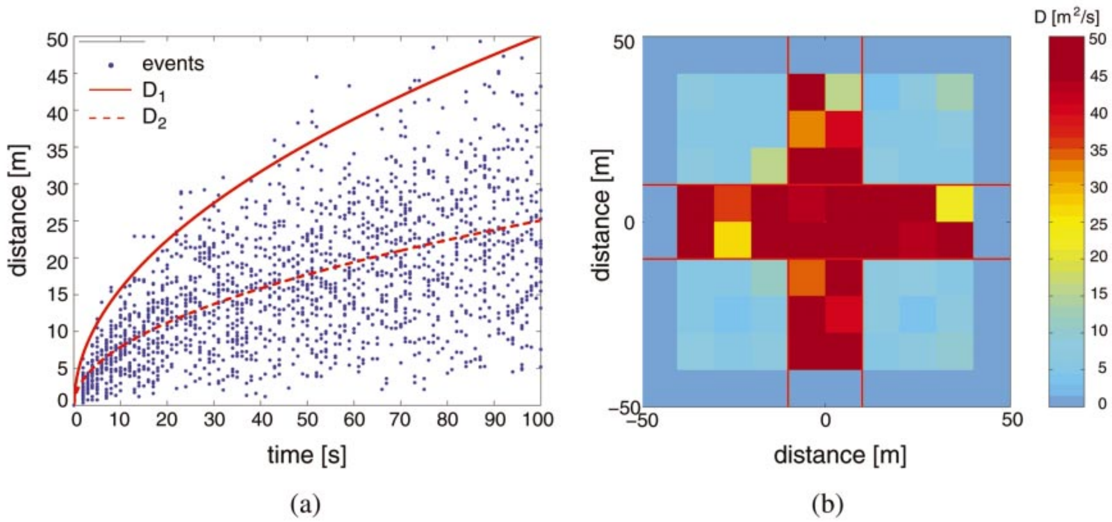

FIG. 5. (a) Estimation of the scalar hydraulic diffusivity using a data set obtained in the model shown in Figure 4a, with $D_1 = 2.0$ m^2/s and $D_2 = 0.5$ m^2/s. The diffusivities have been scaled down for clarity; 99.91% of all events are located below the upper envelope curve. (b) Reconstruction of the diffusivity distribution in the hydraulically heterogeneous model using data shown in Figure 4b and equation (3). The color denotes the magnitude of the diffusivity. The geometry used in the model (indicated by the red lines) is successfully reconstructed. The reconstruction of hydraulic diffusivity in the border regions fails because of boundary effects of the inversion algorithm.

Another important observation obtained using this modeling approach is that there are at least two physically different quantities whose heterogeneous distributions in space strongly influence the appearance of microseismicity clouds. The first one is the triggering critical pressure which we studied. The second is the hydraulic diffusivity. Models with heterogeneously distributed diffusivity are considered in the following section.

NUMERICAL TEST OF THE INVERSION APPROACH

The numerical modeling procedure demonstrated above not only allows us to study the triggering phenomenon within hydraulically homogeneous and isotropic media, but it also provides the possibility to include any desired type of hydraulic model. Media with heterogeneously distributed hydraulic diffusivity can be treated as well as anisotropic ones. In Figure 4a, an example for a simple heterogeneous model is shown. Here, two values of scalar diffusivity are used. The cross-shaped structure is characterized by an increased value of diffusivity ($D_1 = 50$ m^2/s), whereas its value in the surrounding regions is chosen 10 times smaller ($D_2 = 5$ m^2/s). Again, as an input signal a step-function pressure perturbation with constant amplitude in the center of the model is used.

The result of the triggering process is shown in Figure 4b. A total of 20 337 events were triggered during the simulated injection. The estimation of scalar hydraulic diffusivity from this data set obtained in such a type of heterogeneous models is shown in Figure 5a. For clarity of demonstration, we have scaled down the diffusivities to $D_1 = 2$ m^2/s and $D_2 = 0.5$ m^2/s. The coordinates of the events in the space–time domain are shown as blue dots; the curves represent the two values of hydraulic diffusivity used in the model according to equation (2), respectively. It is obvious that even for this model the spatio-temporal structure of the events fulfills the behavior predicted by equation (2); 99.91% of all events are located below the envelope function with $D_{max} = D_1$. Thus, the SBRC algorithm based on equation (2) to estimate maximum scalar hydraulic diffusivity works quite well even for heterogeneous media.

Let us now test the SBRC eikonal equation-based inversion algorithm for reconstructing diffusivity distributions in space.

We reconstruct the distribution of hydraulic diffusivity in the model shown in Figure 4a by applying the SBRC algorithm on the basis of equation (3). The model is subdivided into 10×10 cells, each containing 475 events on average. Triggering time is then defined in each cell, and equation (3) is used directly for estimating D (see Shapiro, 2000; Shapiro et al., 2002). The result of the inversion procedure is shown in Figure 5b. The overall structure (cross shape) of the medium is reconstructed. We also tested the inversion approach on other synthetic models and usually received a well reconstructed distribution of hydraulic diffusivity. This indicates the applicability of the eikonal equation-based inversion [equation (3)] of microseismic data.

CONCLUSIONS

The main hypothesis of the SBRC method is that fluid-induced microseismicity is triggered by a diffusive process of pore-pressure relaxation in subcritically stressed rocks. Using this hypothesis, we have developed a simple numeric model for simulating the space–time distribution of injection-induced microseismicity that depends on hydraulic properties and the statistics and spatial distributions of trigger criticality. The forward model results show time–distance distributions of microseismicity similar to observed microseismic clouds. This similarity supports the idea that pore-pressure relaxation is an important mechanism for triggering microearthquakes. We applied numerical simulations to test the inversion approaches of the SBRC method. We showed that if the hypothesis of the SBRC approach is valid, then the eikonal equation-based inversion method can be used successfully to reconstruct hydraulic properties of rocks from spatio-temporal evolutions of clouds of microseismic events.

ACKNOWLEDGMENTS

This work was supported in part from the sponsors of the Wave Inversion Technology (WIT) university consortium project and in part from the Deutsche Forschungsgemeinschaft through grants SH 55/2-1 and SH 55/2-2.

REFERENCES

Adushkin, V. V., Rodionov, V. N., and Turuntaev, S., 2000, Seismicity in the oil field, Oilfield Rev., **1**, 2–17.

Audigane, P., Royer, J.-J., and Kaieda, H., 2002, Permeability characterization of the Soultz and Ogachi large-scale reservoir using induced microseismicity: Geophysics, **67**, No. 1, 204–211.

Biot, M. A., 1962, Mechanics of deformation and acoustic propagation in porous media: J. Appl. Phys., **33**, 1482–1498.

Cornet, F. H., 2000, Comment on 'Large-scale *in situ* permeability tensor of rocks from induced microseismicity' by S. A. Shapiro, P. Audigane and J.-J. Royer: Geophys. J. Internat., **140**, 465–469.

Dvorkin, J., and Nur, A., 1992, Filtration fronts in pressure compliant reservoirs: Geophysics, **57**, 1089–1092.

Fehler, M., Jupe, A., and Asanuma, H., 2001, More than cloud: New techniques for characterizing reservoir structure using induced seismicity: The Leading Edge, **20**, No. 3, 324–328.

Hubbert, M. K., and Rubey, W. W., 1959, Role of fluid pressure in mechanics of overthrust faulting: Geol. Soc. Am. Bull., **70**, 115–166.

Maxwell, S. C., Young, R. P., Bossu, R., Jupe, A., and Dangerfield, J., 1998, Microseismic logging of the Ekofisk reservoir: Petro. Eng./Internat. Soc. Rock Mech., Eurock 1998 Conf., SPE Paper 47276.

Pearson, C., 1981, The relationship between microseismicity and high pore pressures during hydraulic stimulation experiments in low permeability granitic rocks: J. Geophys. Res., **86**, 7855–7864.

Phillips, W., House, L., and Fehler, M., 1997, Detailed joint structure in a geothermal reservoir from studies of induced microearthquake clusters: J. Geophys. Res., **102**, No. B6, 11,745–11,763.

Rothert, E., Shapiro, S. A., and Urbancic, T., 2001, Microseismic reservoir characterization: Numerical experiments and case studies: 71st Ann. Internat. Mtg., Soc. Expl. Geophys., Expanded Abstracts, RC 2.4.

Rutledge, J. T., Phillips, W. S., and Schuessler, B. K., 1998, Reservoir characterization using oil-production-induced microseismicity, Clinton County, Kentucky: Tectonophysics, **289**, 129–152.

Shapiro, S. A., Audigane, P., and Royer, J.-J., 1999, Large-scale in situ permeability tensor of rocks from induced microseismicity: Geophys. J. Internat., **137**, 207–213.

Shapiro, S. A., Huenges, E., and Borm, G., 1997, Estimating the crust permeability from fluid-injection-induced seismic emission at the KTB site: Geophys. J. Internat., **131**, F15–F18.

Shapiro, S. A., Rothert, E., Rath, V., and Rindschwentner, J., 2002, Characterization of fluid transport properties of reservoirs using induced microseismicity: Geophysics, **67**, 212–220.

Shapiro, S. A., Royer, J.-J., and Audigane, P., 2000, Reply to comment by F. H. Cornet on 'Large-scale in situ permeability tensor of rocks from induced microseismicity': Geophys. J. Internat., **140**, 470–473.

Talwani, P., and Acree, S., 1985, Pore pressure diffusion and the mechanism of reservoir-induced seismicity: Pure Appl. Geophys., **122**, 947–965.

Urbancic, T. I., Shumila, V., and Rutledge, J. T., and Zinno, R. J., 1999, Determining hydraulic fracture behavior using microseismicity: 37th symposium, U.S. rock mechanics, Proceedings, 991–996.

Zoback, M., and Harjes, H.-P., 1997, Injection induced earthquakes and the crustal stress at 9 km depth at the KTB deep drilling site: J. Geophys. Res., **102**, No. 18, 477–492.